HiSST: 2nd International Conference on High-Speed Vehicle Science Technology

11–15 September 2022, Bruges, Belgium

Critical Analysis of SpaceX's Next Generation Space Transportation System: Starship and Super Heavy

Jascha Wilken, Martin Sippel, Michael Berger

German Aerospace Center (DLR), Institute of Space Systems,
Robert-Hooke-Straße 7, 28359 Bremen, Germany

Abstract

For the first time in the history of spaceflight a fully reusable launch system appears possible within the near future. Since its presentation in 2016 SpaceX's next generation space transport system has gone through multiple names and design iterations but some key design features remained constant: Full reusability, Full-Flow Staged Combustion engines and deeply subcooled LOX/LCH4 as propellants.

The current design iteration is of special interest because hardware is being integrated and the first test flights, including landings, of the upper stage have been completed. A key feature of this iteration is the novel approach to use a "skydiving" maneuver to dissipate as much energy as possible through aerodynamic forces before initiating a landing burn and landing vertically.

The implications of a fully reusable system of this size on the orbital launch market are significant even if the ambitious plans for quick turnaround of stages are not fulfilled right from the beginning.

Within this paper, the two-staged system is analyzed from a technical perspective based on publicly available information. The principal goal is to form an understanding of the high-level system properties. Of special interest are the return methods, which exhibit some novel properties. Overall a reasonable agreement between the generated models and the publicly available information is found. The design and its driving factors are discussed and a fundamental understanding of the high-level properties of the system is attained.

Keywords: SpaceX, FFSC, Starship, trajectory, RLV

Nomenclature

CFD	Computational Fluid Dynamics
CoG	Centre of Gravity
DLR	German Aerospace Center
ELV	Expendable Launch Vehicle
FFSC	Full flow staged combustion
Isp	Specific Impulse
ITS	Interplanetary Transport System
LCH4	Liquid methane
LOX	Liquid oxygen
RLV	Reusable Launch Vehicle
RPA	Rocket Propulsion Analysis
RTLS	Return to Launch Site
SLME	SpaceLiner Main Engine

1. Introduction

Since its presentation in 2016 SpaceX's next generation space transportation system has gone through multiple names as well as design iterations but some key design features remained constant: Full reusability, Full-Flow Staged Combustion engines and deeply subcooled LOX/LCH4 as propellants. Other features have changed: While the initial Interplanetary Transport System (ITS) was supposed to weigh over 10,000 tons[1], the current design is projected to weigh about half of that. The main structure material was also changed from carbon fiber composites to stainless steel. The aerodynamic configurations have also been adapted and refined throughout the six years since the initial public presentation. An interim version, the BFR, has also been previously analyzed with similar approaches as will be done herein for the current iteration[7].

The current status, dubbed Starship and Super Heavy [2], is the first where significant progress with regard to hardware integration of entire stages has been achieved. While it is practically certain that the design will be further adapted and refined based on the first orbital tests, the current design is set to be the first fully integrated version that will attempt to reach orbit.

In parallel to the work done on the vehicle systems, the engine development has been progressing quickly. The propulsion development was initially planned to be completed at the end of 2019 [1] and indeed the very first hops of the "Starhopper" test vehicle in that year used functional Raptor engines, making the Raptor the first Full-Flow Staged Combustion-cycle (FFSC) engine ever to be flown.

However, the development continued and the design of the Raptor was further refined, culminating in the current Raptor 2 engine [3], with improved cost, robustness, mass as well as an increased thrust level. Further improvements have also already been discussed publicly.

Within this paper, first the performance of Raptor 1 and 2 are assessed and discussed in section 2.1. The mass model is shown in section 2.2 and the aerodynamic models briefly discussed in section 2.3. Finally, the performance for orbital missions for both ELV and RLV mode are presented in section 3, including the reentry of both stages.

1.1. Goals of the analysis

The primary purpose of this analysis is not a feasibility check on SpaceX's technical design. The company has successfully demonstrated its ability to disrupt the technical and economic status quo of the launch market. While the technical side of the Falcon 9 and its reuse have been analyzed extensively previously [15], the Starship system is based on many unique and unprecedented features. This analysis aims to understand and retrace the design of the Starship launch system as well as gain a fundamental understanding of the return methods used including their benefits and limitations.

As mentioned in the previous section, the design of the Starship system and its predecessors has been highly iterative und it is unlikely that the current iteration will remain unchanged. This analysis was based on the currently available status and information in July 2022. Newer developments were not considered.

2. Modelling the launch system

In this chapter the models generated for propulsion, propellant management, mass and aerodynamics are presented and discussed.

2.1. Propulsion

The SpaceX Raptor (shown in Fig 1), which has already performed several flight tests in atmospheric conditions, operates in a FFSC similar to the SLME (see ref. [10]). Raptor is the first FFSC rocket engine ever flown. The early Raptor's sea-level or booster stage version has a nozzle expansion ratio of 35 and a chamber pressure of at least 250 bar but in latest testing it has been reaching 300 bar and more. The Raptor engine has been previously analyzed by DLR [7], the results with regard to engine performance are shown in Table 1 together with the data given by SpaceX in [1].

Fig 1. SpaceX Raptor engine with booster type (left) and upper stage (right), from [4]

Table 1. SpaceX Raptor Engine technical data, [1] and [7]

	First stage		Upper stage	
	DLR calc. [7]	[1]	DLR calc. [7]	[1]
nozzle area ratio [-]	35		115	
Mixture ratio [-]	3.6		3.6	
Chamber pressure [MPa]	25	25	25	25
Mass flow engine [kg/s]	530.5		530.5	
Specific impulse in vacuum [s]	354	356	374	375
Specific impulse at sea level [s]	326.5	330	285	
Thrust in vacuum engine [kN]	1841		1947	1900
Thrust at sea level engine [kN]	1700	1700	1484	

Since 2022 the new Raptor 2 version is in production for which the nominal chamber pressure has been raised to 30 MPa while the nozzle expansion ratio is slightly reduced. Obviously, the key-objective for this design choice is to significantly increase available thrust on the booster stage while still being able to fit 33 engines in the available Super Heavy diameter. As visible in Fig 2 almost no space is available between the engines and for this reason the outer ring Raptors are not foreseen for gimballing.

Precise engine performance data of the Raptor 2 has not been published. Wikipedia [9] collects some references and combines those into a single table. However, such data collection usually contains several inconsistencies or contradictions. Therefore, an independent DLR-analysis of Raptor 2 has been performed using the rocket cycle calculation tool RPA [6]. The announcement of 230+ tons of thrust[3], the chamber pressure of 30 MPa and nozzle expansion ratio of 34.34 [9] serve as guidelines. Table 2 lists key performance data of Raptor 2 under these assumptions. Data in the Wikipedia column printed in italics and with "?" are based on a combination with other information but are not reliable. For example, a vacuum Isp of 360 s for Raptor is definitely inconsistent with the nozzle area ratio and can't be achieved by a methane engine with these parameters.

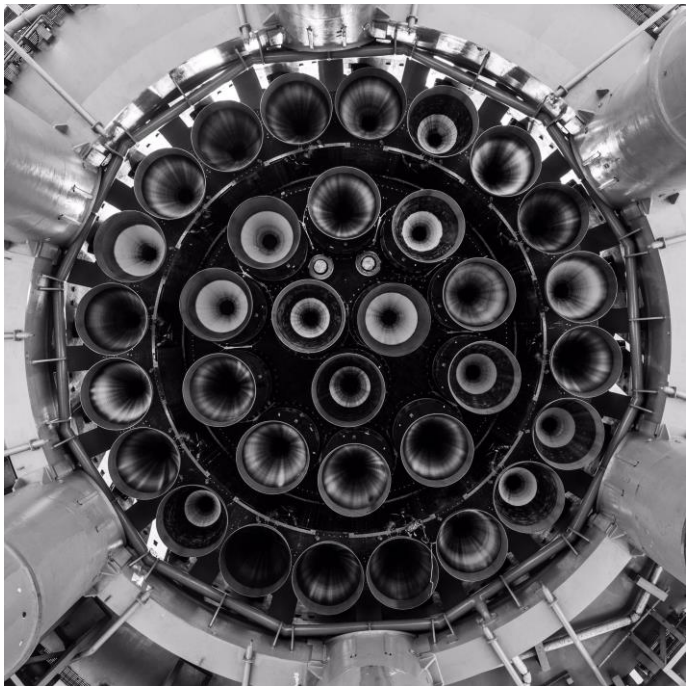

Fig 2. Highly dense mounting of first-generation Raptor on Super Heavy aft section, from [5]

Table 2. SpaceX Raptor 2 Engine technical data

	DLR calc.	DLR calc.	[9]
nozzle area ratio [-]	34.34		
Mixture ratio [-]	3.4	3.6	3.6
Chamber pressure [MPa]	30		
Mass flow engine [kg/s]	681.89	698.2	650
Specific impulse in vacuum [s]	351.5	348.6	*360?*
Specific impulse at sea level [s]	328.7	326	327
Thrust in vacuum engine [kN]	2350	2350	2300
Thrust at sea level engine [kN]	2198	2198	*2085?*

However, a slight variation on the thrust assumptions delivers a range of realistic data and stays in overall good agreement with public announcements. In the left column of Table 2 an engine mixture ratio of 3.4 has been assumed which is close to the optimum with regard to vacuum Isp with a small shift to the right. If the mixture ratio is set to 3.6 following [9] the Raptor 2 Isp drops by at least 2.5 s with almost identical thrust. This degradation in engine performance could make sense from a launcher system perspective. Increasing the fraction of oxygen allows the storage of more propellant in the same tank volume and hence the total impulse of the stage might increase despite a slightly reduced average Isp. Raptor 2 is capable of operating in both mixture ratio conditions and might actually do so depending on the specific mission. The two columns of DLR calculations define the likely range of practical Raptor 2 performance at full-thrust-level. Reducing the MR below 3.4 would significantly decrease the available propellant loading, exceeding the MR beyond 3.6 would hurt the performance because of the resulting Isp-loss. All DLR calculations are based on the thrust-sizing assumption of 2200 kN to be delivered at sea-level conditions.

2.2. Mass model

The dry mass of both stages was estimated using the in-house tool *stsm* based on empirical formulas derived from previously built and flown components of historical stages. The geometric dimensions of the Starship SN8 were used as a basis and derived from the pictures available online [12]. The core geometric dimensions are shown in the following Table 3.

Table 3. Main geometric parameters

Starship	Length	50 m
	Diameter	9 m
	Volume LOX main tank	790 m³
	Volume LCH4 main tank	590 m³
	Volume LOX header tank	19 m³
	Volume LCH4 header tanks	17 m³
Super Heavy	Length	70 m
	Volume LOX main tank	2251 m³
	Volume LCH4 main tank	1700 m³

Since the thickness of the steel sheets used for the early protypes is known and confirmed by Elon Musk [11], the mass resulting from the empirical formula was cross checked with the mass resulting from the calculation of the structure volume. For the main tanks the values are within ~5% of each other, a good agreement considering the simplistic nature of each estimation [12].
The tank and feedline geometries were analyzed with the in-house tool *pmp*. In order to fit the announced amount of propellants into the available space, a densification down to almost 90 K for the LCH4 and almost 60 K for the LOX is necessary, which is in line with SpaceX's announcement of using "deep cryo" propellants. The propellant loadings are taken from [2].

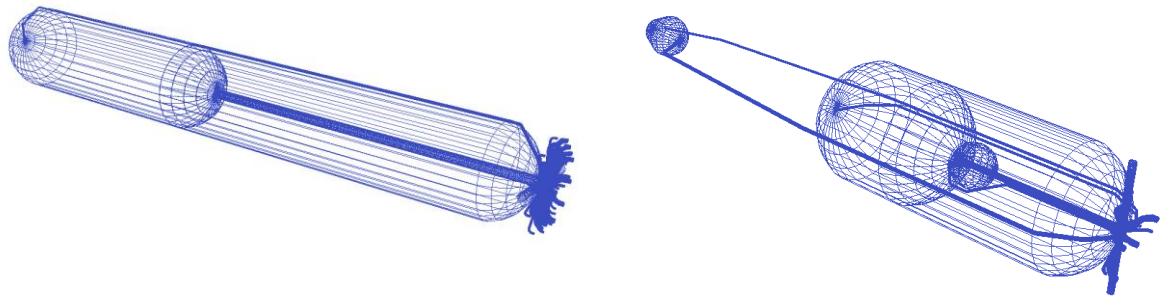

Fig 3. Tank and propellant supply model for Super Heavy (left) and Starship (right) stages

A 14% mass margin was applied to all subsystems due to the novel nature of the design and the preliminary nature of the analysis tools. For the propulsion system the margin was reduced to 12% since that is the subsystem where the analysis has the highest confidence due to the worldwide heritage with hydrocarbon-based engines. However, due to the limited experience with methane itself the margin was not reduced further. The mass budget, and the following mission analysis, assume 33 Raptor 2 engines on the first stage as well as three Raptor 2 and three (large expansion ratio) Raptor 1 engines on the second stage.
The dry masses used in the following trajectory analysis are summarized in the following Table 4:

Table 4. Summary of mass model of Starship and Super Heavy

First stage (Super Heavy)	Propellant mass	3400 t
	Dry mass	270 t
	Total mass	3670 t
	Structural index (w engines)	7.9 %
	Structural index (wo engines)	4.8 %
Second stage (Starship)	Propellant mass	1200 t
	Dry mass	130 t
	Total mass	1330 t
	Structural index (w engines)	10,6 %
	Structural index (wo engines)	8,9 %
Vehicle	Total mass (without payload)	4997 t

Usually, previously built stages could be used for a cross check of the mass estimation but multiple factors make this difficult. For one, no orbital system with methane as fuel has been flown (up to now) so the only comparison possible is to stages with other fuels (hydrogen or kerosene) and secondly the magnitude of the stages is also beyond the previously seen scope. And especially for the Starship, the stage architecture itself is also new, so that the comparison to other upper stages is hardly useful. The values arrived at within this analysis are higher than target values announced by SpaceX, but not extraordinarily so. A core goal of future design iterations will be the reduction of the dry mass, being one the main parameters for optimizing the performance of the system, especially for the second stage. And while lower values might be targeted by SpaceX, that does not necessarily mean that they are also achieved in the first generation of integrated vehicles.

2.3. Aerodynamic properties

For both stages aerodynamic models were generated using DATCOM based semiempirical engineering methods [12]. In total, aerodynamic coefficients had to be generated for three configurations:

- Full configuration for Ascent
- Descent configuration for the Super Heavy Booster
- Descent configuration for Starship

The model for the Super Heavy booster was substantially simplified, the chosen semi empirical methods are not able to correctly account for the complex geometries of the engines pointing forward during the return flight. The aerodynamic properties were crosschecked with computational fluid dynamics (CFD) calculation from similar configurations [13]. However, due to difference in size and shape a certain amount of uncertainty remains.
While the aerodynamic properties of the upper stage are not critical for the performance of the vehicle, they are critical for the safe return end efficient reuse of the vehicle. An extensive investigation of pitch trim was performed [12]. Since the Starship has two pairs of flaps, multiple combinations of flap deflection lead to a trimmed state for a given aerodynamic state. Within the mission analysis, multiple options for selecting the ideal flap deflection for each aerodynamic state were assessed, the results of this are summarized within section 3.3. The results were compared to the similar investigation of pitch trim done for a previous Starship iteration[14] and found to be in good agreement[12].

3. Mission analysis

The primary purpose of the Starship launch system is the transport of an enormous amount of payload into low earth orbit. While initially the payloads will probably primarily be Starlink satellites, the ultimate goal is the refueling of transport ships to Mars. Thus, within this analysis the focus is on the ascent to LEO with a fully reusable launch system and the return of both stages to Earth.

While the full optimization of the trajectories for descent and ascent are done separately, the amount of propellant needed for descent is estimated within the ascent trajectory simulation. This enables the ascent optimization to find a compromise between ideal initial conditions for the Return-to-Launch-Site (RTLS) maneuver and the needs for sufficient horizontal acceleration during ascent. The Δv budget estimation for the boostback is done with analytical formulas. It is assumed that the boostback burn only neutralizes the horizontal velocity and adds a component towards the launch site that is sufficient for the stage to be over the launch site when it reenters the atmosphere. For the final landing and hovering phase next to the launch tower 600 m/s Δv budget is assumed. This budget includes the ability to slowly descent or hover next to the launch tower for 10 seconds on top of the Δv necessary to counteract the final falling speed of the Super Heavy stage.

After an optimal trajectory for ascent is found, using this simplified estimation for descent propellant, the descent trajectory is also integrated and optimized with the in-house tool *tosca*. It was found that the estimated descent propellant budget was within a percent of the values resulting from the full optimization. However, this value is dependent on first deriving an approximate final falling speed of the stage at ignition of the landing burn.

3.1. Ascent into LEO

The mission into LEO was evaluated for two cases: The maximum payload possible as an ELV or with full reusability. In the RLV case, a significant amount of Super Heavy propellant is not burned upon

ascent but is used to neutralize the horizontal velocity away from the launch site and for landing the stage.

For these trajectories it was assumed that all six engines of the second stage continue firing until second stage engine cut-off. While the vacuum optimized engines by themselves do not have sufficient thrust to bring the second stage and a significant payload to orbit completely by themselves, it seems feasible to shut down the sea-level engines at some point during the second stage ascent. This degree of freedom was not investigated herein and would likely provide some additional payload performance due to the higher Isp of the vacuum optimized engines.

- The following boundary conditions were used for the ascent trajectory simulation:
- Launch from Boca Chica
- Target orbit: 200km circular orbit at 26° inclination

The payload performance for both the ELV and RLV case, calculated based on the models shown in the previous sections, are given in Table 5.

Table 5. Estimated payload capacity of Starship Launch system into a 200x200km orbit at 26° inclination

ELV payload	204 t
ELV mass to orbit	343 t
RLV payload	90 t
RLV mass to orbit	268 t

It can be seen that the payload is reduced substantially by reserving propellant for the safe return of the stages. It can also be seen that contrary to systems with multiple stages and a small upper stage the majority of the mass brought into orbit is not payload but the dry mass of the second stage as well as residuals, reserves and the propellant needed for landing of the second stage. Thus, the total reduction of mass inserted into orbit is only 22 %, while the payload itself is reduced by 56 %. This payload penalty is of course offset by the ability to reuse the launch vehicle.

The payload performance for the RLV case is lower than the values given by SpaceX (over 100 t with full reusability [2]). The most likely cause is the difference in the dry masses of the stages, especially the second stage. The resulting trajectories for ascent of both ELV and RLV missions as well as the RTLS of the first stage are shown in the following Fig 4.

For the ascent two differences between the mission as an ELV and RLV can be seen: Firstly, the shorter operation time of the first stage, due to the propellant reserved for the boostback and landing burns and secondly the slightly steeper ascent for the RLV mission. This is done in order to find a compromise between the optimal ascent trajectory and the boostback maneuver. The Δv demand for the boostback burn is dominated by the need to neutralize the horizontal velocity away from the launch site, so it is beneficial to have the stage separation at higher flight path angles. However, the general goal of the ascent trajectory is essentially the generation of sufficient horizontal velocity to achieve the desired orbit, flying steeper than necessary increases the gravitational losses. As can be seen the compromise between these goals leads to the aforementioned slightly steeper ascent.

The maximum acceleration was not limited and thus reaches almost 6g during the final seconds of the ascent, it might be necessary to throttle the engines at this point in order to reduce the loads on the payload, but since this only affects the final portion of the ascent, the performance impact is not expected to be large.

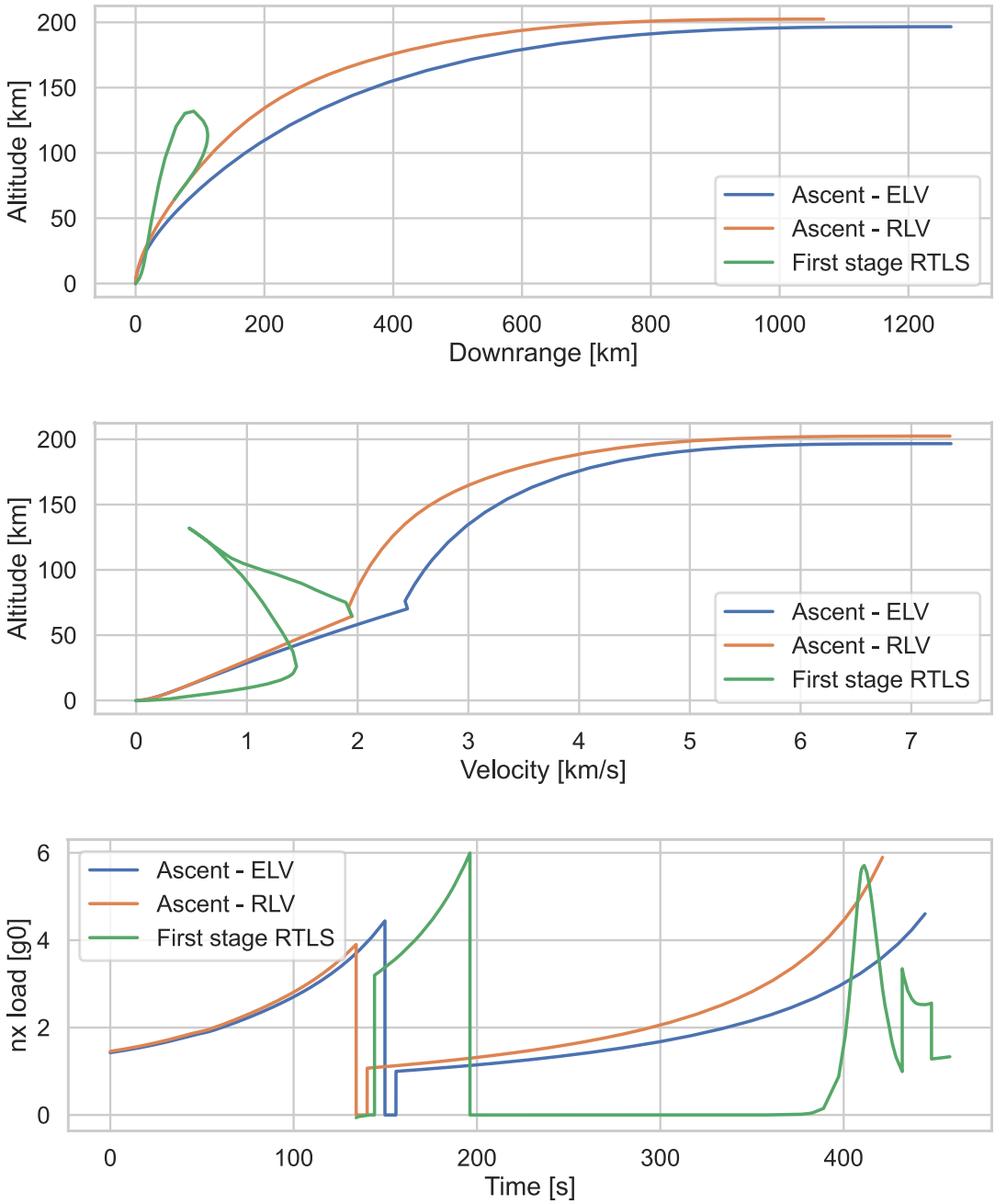

Fig 4. Main parameters of the trajectory as ELV and RLV

3.2. Return to Launch Site of Heavy Booster

In principle, the general method for the RTLS of the Super Heavy booster is the same as for the equivalent missions of the Falcon 9, with two main differences:

- No landing legs: Instead of using deployable landing legs as done with the F9, the launch tower contains movable segments to "grab" the hovering stage and carry the weight after extinguishment of the engines
- Increased ballistic coefficient: The Falcon 9 has a diameter of 3.6 m and a landing mass of roughly 20t [15], the SH has a diameter of 9 m, but solely the dry mass is estimated within this work to be 270 t. Thus, the ballistic coefficient, assuming an identical drag coefficient, is a factor of two higher.

The omission of landing legs only has a small impact on the descent trajectory, the final point at which the velocity shall be close to zero will now be slightly above the Earth's surface. For this reference scenario, a 10 second hovering phase is also modelled, as mentioned in [16].

The second point, the higher ballistic coefficient does have a noticeable impact on the trajectory. Essentially, this makes it harder to use the atmosphere for breaking. In order to still decelerate as much as possible through aerodynamic forces, design changes will be necessary. Any deceleration that can not be done through aerodynamic means has to be provided via the engines. This is undesirable from an efficiency point of view, since that is propellant that could be used for acceleration of the first stage during ascent. Any additional propellant needed for the landing burn also inherently causes additional propellant needed for the boostback maneuver, in essence increasing the inert mass for that maneuver.

In order to avoid this cost, the aerodynamic forces can be increased. This can be done by changing or increasing the aerodynamic shape or by flying at higher angles of attack. This seems to have been the motivation for adding chines to the Super Heavy stage. According to SpaceX they increase the pressure on the vehicle surface as well as allow it to fly at higher angles of attack by shifting the center of pressure closer to the center of gravity [16].

In order to truly assess the effect of the chines on the aerodynamic performance extensive analysis via CFD would be necessary, which is outside of the scope of this analysis. Instead the range of allowed angle of attacks is increased to +/-20° during the final portion of the RTLS. This might be larger than will be actually flown by SpaceX, but this can be seen as a surrogate for the additional lift and drag caused by the chines which are not accounted for within the simplified aerodynamic models. For future studies a parametric variation of, for example, the reference area would be of interest in order to exactly quantify the effect of increased or decreased ballistic coefficient.

Even with these large angles of attack the dynamic pressure encountered by the returning stage is substantially higher than during ascent (~35 kPa vs over 200 kPa). The lift generated by the higher angles of attack is enough to generate lateral accelerations of over 4.5 g. It is expected that the sizing loads for the stage nonetheless occur during the ascent of the vehicle, since the vehicle is empty at this point. Even though the lateral acceleration is high, the actual forces are not necessarily as high as during ascent. This has been shown for a winged stage in [17], which experiences similar lateral loads.

In a trajectory optimized with these assumptions the engines are ignited at about Mach 1 for the landing burn. In [16], it is mentioned by SpaceX that the ignition is projected to be at Mach 0.5. This discrepancy is either caused by a difference in the aerodynamic properties of the vehicles or a difference in the assumed landing mass. As mentioned in 2.2, the mass estimations for the first stage are more conservative then the target values mentioned by SpaceX. Due to the relatively simple approach used for the modelling the effect of the chines, it also is possible that their beneficial effect is being underestimated. Both of these factors will have a direct impact on the final falling speed and thus the amount of propellant needed for the landing burn.

3.3. Reentry of Starship

The upper stage, Starship, uses a novel approach to efficiently decelerate from orbital velocities and subsequently land: the so-called skydive maneuver. The phases of this type of reentry are shown in Fig 5.
During the initial entry into the atmosphere, the primary goal is the reduction of the maximum heat flux, this is done by maximizing the drag at higher altitudes, so that as much velocity as possible is shed at high altitudes without generating excessive heat loads. While drag is the primary focus in this phase, additional lift can also help the vehicle fly a shallower trajectory, again enabling more velocity to be shed before entering the denser parts of the atmosphere. Thus, an extremely high angle of attack (70°) is chosen for this phase [19].

During the subsonic "skydiving" portion, the goal is to safely reach terminal velocity. Ideally this terminal velocity is as low as possible, reducing the propulsive need for the landing. During this phase the Starship flies with essentially 90° angle of attack, maximizing the drag and thus achieving a comparatively slow terminal velocity.

As mentioned in section 2.3, the Starship design currently includes four movable wings/flaps. Within this analysis only pitch trim was considered, it was assumed that the system is stable with regard to roll and yaw. Since the vehicle has two sets of flaps, multiple combinations of flap deflection lead to

trimmed states. This necessitates the definition of a selection criteria in order to arrive at an optimal trimmed aerodynamic dataset. Thus, for a given aerodynamic state (Mach number and angle of attack) the combination of flap deflections was selected that lead to the highest drag coefficient while still being trimmed. The possibility of optimizing the trimmed states for highest lift-to-drag ratio was also investigated but lead to higher heat loads during reentry [12].

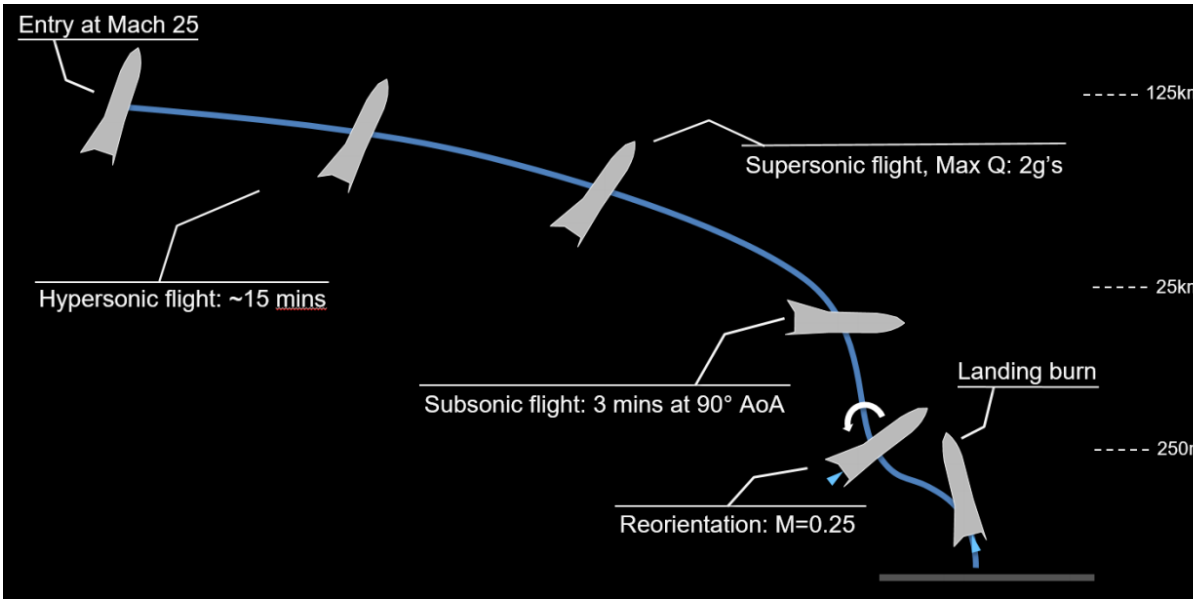

Fig 5. Phases of reentry for the SpaceX Starship, from [18]

While the exact position of the center of gravity (CoG) for the system is not known (and will vary depending on the position and mass of the payload) the simplified aerodynamic database was used to identify CoG positions at which the configuration can be trimmed in the hypersonic regime. In that regime the limiting factor was trimability at high angles of attack (~70). It was found that the stage can be pitch trimmed at that point if the CoG is between 43% and 59% of the vehicle length. Compared to other reentry configurations this is a quite large range, which allows for some flexibility. This flexibility might be needed since it is expected that the stage will land with and without payload, and since the payload is in the same order of magnitude of the stage dry mass it will have significant impact on the CoG position.

However, it should be noted that the trimmed states for more backward CoG positions allow for more effective flap surface area to be exposed to the flow, which results in higher drag coefficients, effectively reducing the heat flux encountered during reentry by ~9% when compared to the cases with a more forward CoG position [12].

As another degree of freedom, the propellant in the header tanks will also influence the CoG position, and it seems feasible to adapt the propellant loading of the tanks from mission to mission in order to further optimize the CoG position and the resulting aerodynamic properties.

Based on the aforementioned propulsion, mass and aerodynamic models, the descent of the Starship from LEO was simulated with the in-house trajectory optimizer *tosca.* Two cases were simulated, the descent of the Starship loaded with 130t of payload as well as a descent without any payload. The initial conditions of the descent simulation are shown in Table 1.

Table 1: Initial conditions for Starship re-entry simulation

Altitude	100 km
Flight path angle	-1°
Velocity	7.419 km/s

The reorientation maneuver, with which the Starship is reoriented for landing, was approximated as an instantaneous event since the vehicle is modelled as a point mass within this simulation. For a full evaluation of the flip maneuver, an evaluation with a full six degrees of freedom simulation is necessary,

which necessities additional aerodynamic datasets as well as an estimation of the inertia tensor of the vehicle.

The resulting trajectory is shown in Fig 6 below. The heat flux values refer to the stagnation point heat flux according to a modified Chapman equation as shown in formula (4). Here, ρ is the local density at the respective altitude according to the US standard atmosphere 1976, ρ_R is a reference density value of 1.225 kg/m³, $R_{N,r}$ is reference nose radius (here 1 m), R_N is the vehicle nose radius (here 4.5 m), v is the vehicle's velocity and v_R is a reference velocity of 10000 m/s.

$$\dot{q} = \mathbf{20254.4}\, W/cm^2 \cdot \sqrt{\frac{\rho}{\rho_R}\frac{R_{N,r}}{R_{,N}}}\left(\frac{v}{v_r}\right)^{3.05} \tag{4}$$

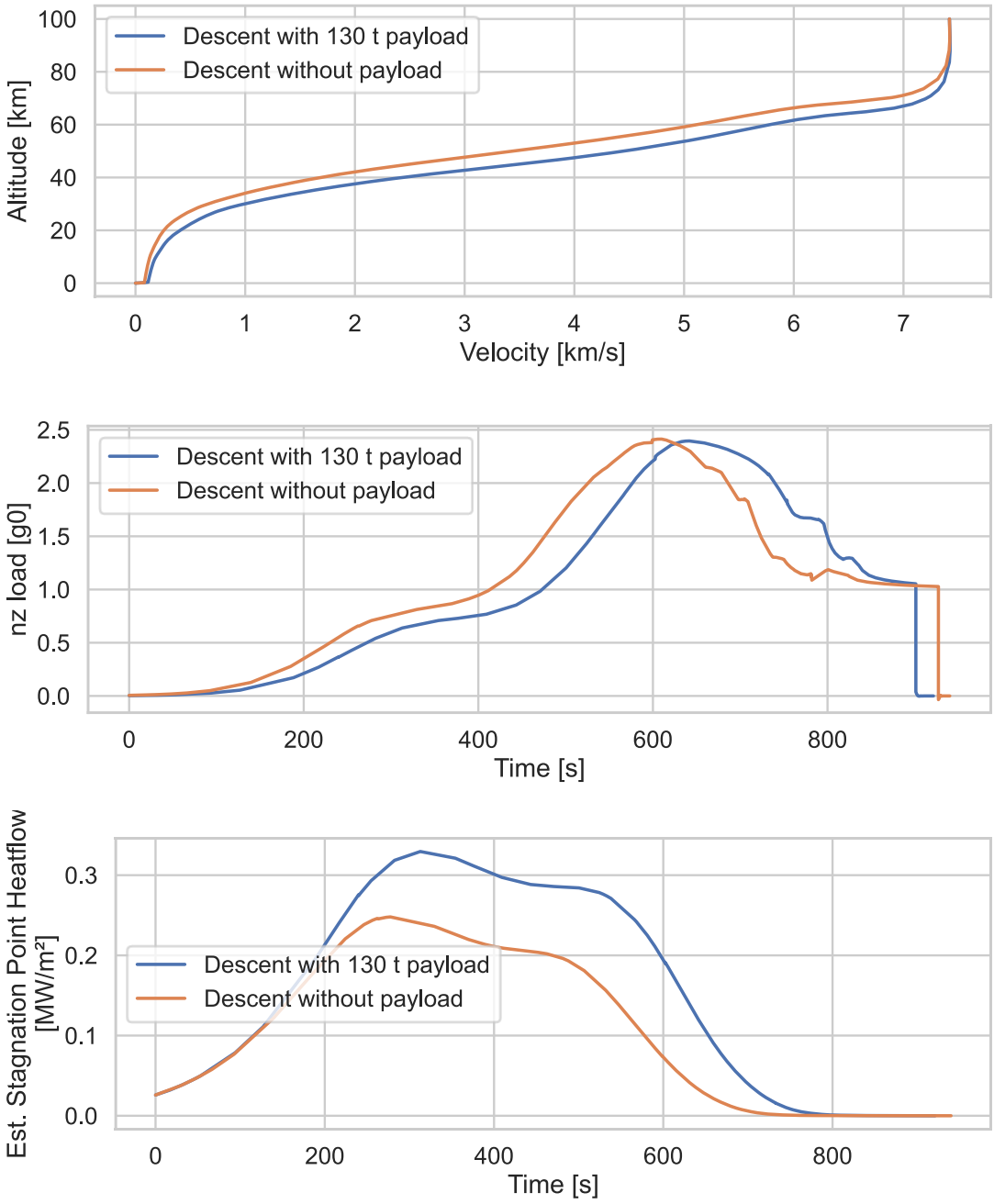

Fig 6. Reentry trajectory of Starship

As can be seen in the reentry profile, the vast majority of the stages kinetic energy is dissipated through aerodynamic forces, only a small portion is done with propulsion. This is limited to the landing burn, which for the case without payload is initiated at about 70 m/s and with payload is initiated at 110 m/s. The value without payload is in good agreement to the value of 67 m/s shown by SpaceX [19].

As can be seen in Fig 6 the stage with payload enters significantly deeper into the atmosphere at higher velocities which in turn leads to the higher heat fluxes. While the maximum value of ~0.3 MW/m² is not excessively high for an orbital reentry, this value was calculated for a theoretical nose radius of 4.5m, which corresponds to the diameter of the cylindrical part of the vehicle. The local heat fluxes on smaller protrusions, for example the flaps, will be much higher.

The mechanical loads are expected to be benign, and well within the range tolerated by humans, even untrained passengers, with the maximum lateral acceleration staying below 2.5g.

3.4. Point-to-Point missions

The full reusability of the Starship launch system could enable a new class of commercial transport missions: Point-to-Point missions for long distance travel on earth. This new class of mission is outside the scope of this paper but is part of currently ongoing further analysis and will be discussed in forthcoming publications [20].

4. Conclusion

For the Starship launch system models have been generated for propulsion, propellant management, aerodynamics, mass budget as well as the ascent and descent trajectories of both stages based on publicly available information. These models were used to assess the performance of the system as an RLV and ELV into LEO. The resulting payload performance is slightly lower than the value given by SpaceX, however not critically so. Overall, the models generated within this analysis and the information available are in reasonable agreement increasing the confidence that the system has been modelled well enough and its fundamental properties understood.

The operational and economical challenges of scaling up the number of launches to the order of magnitude envisioned by SpaceX were not within the scope of this study. However, even if the system does not achieve the planned flight rate quickly, the sheer amount of payload capacity added to the orbital launch market is expected to be highly disruptive.

The next step of the technical analysis is the further assessment of the rocket-propelled Earth-to-Earth missions possibly made economically feasible through the full reusability of the Starship system.

Acknowledgements

Part of this work was performed within the project 'European Concept of Higher Airspace Operations' (ECHO). This project has received funding from the SESAR Joint Undertaking (JU) under grant agreement No 890417. The JU receives support from the European Union's Horizon 2020 research and innovation programme and the SESAR JU members other than the Union. Further information on ECHO can be found at https://higherairspace.eu/

References

[1] Musk, E.: Making Life Multiplanetary. https://www.spacex.com/media/making_life_multiplanetary_2016.pdf, (2016), accessed August 2022

[2] SpaceX: Starship, https://www.spacex.com/vehicles/starship/, accessed August 2022

[3] SpaceX: Starship Update. https://youtu.be/3N7L8Xhkzqo, (2022), accessed August 2022

[4] SpaceX: The first Raptor Vacuum engine (RVac) for Starship has shipped from SpaceX's rocket factory in Hawthorne, California to our development facility in McGregor, Texas. https://twitter.com/SpaceX/status/1302038129990279168, 2020, accessed August 2022

[5] SpaceX: 33 Raptor engines installed on the Booster, 6 on the Ship, https://twitter.com/SpaceX/status/1543289714022678528/photo/1, July 2022, accessed August 2022

[6] Ponomarenko, A.: RPA: Design tool for liquid rocket engine analysis. (2009).

[7] Sippel, M.; Stappert, S.; Koch, A.: Assessment of multiple mission reusable launch vehicles, in Journal of Space Safety Engineering 6 (2019) 165–180, https://doi.org/10.1016/j.jsse.2019.09.001

[8] Musk, E.: Making Life Multi-Planetary, in *NEW SPACE*, VOL. 6, NO. 1, 2018 DOI: 10.1089/space.2018.29013.emu

[9] N.N.: SpaceX Raptor, https://en.wikipedia.org/wiki/SpaceX_Raptor

[10] Sippel, M., Stappert, S., Bayrak, Y.M.; Bussler, L., Callsen, S.: Systematic Assessment of SpaceLiner Passenger Cabin Emergency Separation Using Multi-Body Simulations, 2nd HiSST-conference, Bruges, September 2022

[11] Elon Musk: "Unmodified water tower machines do not work well for orbital rockets…", https://twitter.com/elonmusk/status/1225688871158968324, February 2020, accessed August 2022

[12] Berger, M.: Systemanalyse des SpaceX-Starships inklusive Untersuchung der Skydiving-Rückkehrmethode, SART TN 001/2021, 2021

[13] Stappert, S.; Wilken, J.; Bussler, L.; Sippel, M.; Karl, S.; Klevanski, J.; Hantz, C.; Briese, L. E.; Schnepper, K: (2019) European Next Reusable Ariane (ENTRAIN): A Multidisciplinary Study on a VTVL and a VTHL Booster Stage. In: Proceedings of the International Astronautical Congress, IAC. 70th International Astronautical Congress, 21.10-25.10.2019, Washington DC.

[14] T. Cantou, N. Merlinge and R. Wuilbercq: 3DoF simulation model and specific aerodynamic control capabilities for a SpaceX's Starship like atmospheric reentry vehicle, Madrid, July 2019.

[15] E. Dumont, S. Stappert: Reusability of launcher vehicles by the method of SpaceX, SART TN-007/2016, 2016

[16] Dodd, T.: Go up SpaceX's Starship-catching robotic launch tower with Elon Musk! [Video], YouTube. 2022, https://youtu.be/XP5k3ZzPf_0, accessed August 2022

[17] Wilken, J.; Callsen, S.; Daub, D.; Fischer, A.; Liebisch M.; Rauh, C.; Reimer, T.; Sippel, M: Investigation of insulation of thermal protection systems for reusable cryogenic stages. 2nd International Conference on High-Speed Vehicle Science Technology, 11.-15. September 2022, Bruges, Belgium

[18] elonx.net: Starship Compendium, https://www.elonx.net/super-heavy-starship-compendium, accessed December 2020

[19] SpaceX: Starship Update, Link: https://www.youtube.com/watch?v=sOpMrVnjYeY (2019), accessed August 2022

[20] Callsen, S.; Wilken, J.; Stappert, S.; Sippel, M.: Feasible options for point-to-point passenger transport with rocket propelled reusable launch vehicles, 73rd International Astronautical Congress, 18-22 September 2022, Paris, France